J. Fluid Mech. (2007), *vol.* 582, *pp.* 169–178.
doi:10.1017/S0022112007006398 Printed in the United Kingdom

Finite-amplitude thresholds for transition in pipe flow

J. PEIXINHO AND T. MULLIN

Manchester Centre for Nonlinear Dynamics, The University of Manchester, M13 9PL, UK

(Received 15 February 2007 and in revised form 11 April 2007)

We report the results of an experimental study of the finite-amplitude thresholds for transition to turbulence in a constant mass flux pipe flow. The flow was perturbed using small impulsive jets and push–pull disturbances from holes in the pipe wall. The flux of the disturbance is used to define an amplitude for the perturbation and the critical value required to cause transition scales in proportion to Re^{-1} for jets. In this case, the transition is catastrophic and the scaling suggests a simple balance between inertia and viscosity. On the other hand, the threshold scales as $Re^{-1.3}$ or $Re^{-1.5}$ for push–pull disturbances with the precise value depending on the orientation of the perturbation. Further, the amplitudes required to cause transition are typically an order of magnitude smaller than for jets. When the push–pull perturbation was applied in the oblique direction, streaks and hairpin vortices appeared during the growth phase of the disturbance. The scaling of the threshold and the growth of structures are both consistent with ideas associated with temporary algebraic growth.

1. Introduction

The onset of turbulence in the flow through a long circular straight pipe has intrigued scientists since the original experiments of Reynolds (1883). The problem is simple in concept and yet the origins of the observed turbulent motion remain unclear with the principal issue being that all theoretical and numerical work using classical stability approaches suggests that the flow is linearly stable (Drazin & Reid 1980), i.e. it remains laminar for all Re and yet most practical pipe flows are turbulent. Hence, there is a conflict between standard stability theory and observation. (Here, $Re = UD/\nu$ where U is the mean velocity, D is the pipe diameter, and ν the kinematic viscosity of the fluid.) Recently, significant attention has been paid to the possibility of algebraic growth of small-amplitude disturbances because of the generic non-normal properties of the Navier–Stokes equations. The historical development of these ideas is discussed in Schmid & Henningson (2001) and Schmid (2007) and their impact on transition in pipe flow is reviewed by Kerswell (2005).

Reynolds (1883) found two critical values for which the transition to turbulence occurs. A critical value of $Re = 2260$ was found when experiments were performed using industrial pipes and the mains water supply and a higher value of $Re = 13\,000$ was obtained in a more controlled experiment using precision equipment. Pfenniger (1961) managed to extend the range of laminar pipe flows up to $Re = 100\,000$. Indeed, many other experiments (e.g. by Leite 1959; Wygnanski & Champagne 1973) confirm that the flow is stable to small disturbances. Thus, it is natural to assume that finite-amplitude perturbations are responsible for triggering turbulence and, as Re is increased, a smaller amplitude is required to trigger transition. A question which

may be asked is how does the critical amplitude that can trigger transition scale with Re? This issue has been addressed in several recent studies and quantitative estimates have been provided for pipe flows by Darbyshire & Mullin (1995), Draad, Kuiken & Nieuwstadt (1998) and Hof, Juel & Mullin (2003). Darbyshire & Mullin (1995) used a variety of disturbances including impulsive injection and suction to perturb fully developed Poiseuille flow. They found that the amplitude required to produce turbulence diminishes as the Re increases, but remained finite even at values of $Re \sim 10\,000$. Draad *et al.* (1998) used a porous pipe section to apply periodic suction and injection, and found different scalings depending on the frequency of the disturbance. Hof *et al.* (2003) used a boxcar impulsive disturbance with six small jets arranged azimuthally and found that for a sufficiently long boxcar, the amplitude scales as Re^{-1} over the range $Re \sim 2000$–$20\,000$. (N.B. Extracting exponents directly from the results of Darbyshire & Mullin (1995) is difficult since their perturbation is short and triangular.) A qualitatively similar scaling law for threshold levels was also reported for boundary-layer transition by Govindarajan & Narasimha (1991).

A motivation behind seeking scaling laws is that insights into the transition process can be uncovered, as discussed by Trefethen *et al.* (1993). One difficulty in making a direct comparison between the results of experimental and theoretical investigations is that the amplitude of the physical disturbance cannot easily be related to perturbations used in numerical studies. Direct numerical simulations of pipe flows by Shan, Zhang & Nieuwstadt (1998), Meseguer (2003) and Eckhardt & Mersmann (1999) find scaling laws which suggest Re^{-1} to $Re^{-1.5}$. In all of these investigations, periodic boundary conditions are used with relatively short calculation domains and they therefore cannot capture the observed flow structures such as the puffs studied by Wygnanski & Champagne (1973) in transitional pipe flow in the range $Re \sim 2000$–4000. This issue is discussed by O'Sullivan & Breuer (1994) who argue that the minimum length for the calculation domain is $\sim 30D$ if realistic numerical results are to be obtained over this range of Re. Mellibvosky & Meseguer (2006) studied the effects of streamwise-independent finite-amplitude perturbation and found scaling laws which give relationships of between Re^{-1} and $Re^{-1.5}$ using periodic boundary conditions with calculation domains which were 20 to $100D$ long.

It is clear that the scaling laws discussed above cannot hold for very small Re since the flow is accepted to be globally stable for $Re \lesssim 1800$. A possible method for testing this assumed lower limit of stability would be to inject large-amplitude perturbations into the flow and observe their decay. This method was used by Mullin & Peixinho (2005) to demonstrate that there is a sharp cutoff at $Re \sim 1760$, i.e. below this value, turbulent flow could not be sustained. However, injecting large disturbances into the flow can have significant effects on the mean flow distribution, which can lead to unusually long transient effects (Binnie & Fowler 1948). Further, introducing *ad hoc* disturbances into an infinite-dimensional system is generally questionable and to obviate this difficulty, Peixinho & Mullin (2006) studied the reverse transition, i.e. they investigated the relaminarization of a specific state, the puff. These results have been confirmed in numerical investigations by Willis & Kerswell (2007). Peixinho & Mullin (2006) observed that modulated wavetrains emerge from the long-term transients. They have features which are qualitatively similar to the finite-amplitude travelling waves predicted by Faisst & Eckhardt (2003) and Wedin & Kerswell (2004).

When a detailed study is performed using the impulsive injection of a disturbance, it is observed that the transition process is catastrophic (Darbyshire & Mullin 1995). Ideally, a short duration localized disturbance is desired to test the response of the flow field. Localization can be achieved using a zero net mass flux push–pull system

as shown by Darbyshire & Mullin (1995). However, numerical investigations in jets by Seidel & Fasel (2001) and boundary layers by Levin (2005) and Levin, Davidson & Henningson (2005) have shown the importance of the geometry and orientation of the perturbation. Hence, the strategy we employ here is to use a localized disturbance which could be oriented with respect to the main flow. The hypothesis we wish to test is that the breakdown to turbulence will be less abrupt. Moreover, different orientations of the disturbance might reveal a sequential transition process. Our objective was to carry out a consistent and comprehensive study of the dependence of the transition thresholds and the scaling for the critical amplitude versus Re for different disturbances.

2. Experimental set-up

The pipe had a diameter of $D = 20 \pm 0.01$ mm and was constructed from 105 machined sections 150 mm long which were butted flush so that there was no measurable gap between each section. The total length of the pipe was 15.75 m ($785.5D$) and it was held on a steel backbone and initially aligned using a laser. A reservoir with a capacity of 100 l was connected to the pipe through a smooth trumpet-shaped inlet. A stainless steel cylinder with a bore of 260 ± 0.065 mm and a length of 1180 mm contained a piston of diameter 259.68 ± 0.07 mm mounted on a pair of 12 mm thick lip seals. This device was used to pull the fluid at a constant mass flux along the pipe using a computer-controlled motor and lead screw arrangement. Hence, even if the motion became turbulent, the mass flux through the pipe was unaffected so that Re remained constant.

The facility enabled a laminar flow to be achieved up to $Re = 23\,000$. Poiseuille flow could only be obtained at such high Re when settling times of 1 h were allowed between runs. Estimates of the settling period were established empirically and were presumably related to the decay of any disturbances in the header tank. This underlines the fact that pipe flow is sensitive to inlet disturbances but, once Poiseuille flow has developed, a finite-amplitude perturbation is required to cause transition in practice. The long-term temperature stability of the laboratory was controlled to ± 1 K at a mean temperature of 20 °C. This control of the background environment was also necessary to ensure repeatability. Further details of the experiment can be found in Hof *et al.* (2003), Mullin & Peixinho (2005) and Peixinho & Mullin (2006).

The disturbance was applied 285 pipe diameters from the pipe entrance, which ensured that fully developed flow was established for $Re \leqslant 10\,000$, the maximum value used in the present investigation. As discussed by Darbyshire & Mullin (1995) and Williams (2001), the threshold is probabilistic with a definite distribution so that a mean value can be estimated with a narrow well-defined width. The width of the distributions was used to define the error bars indicated on the estimates of the thresholds.

The disturbance generator (figure 1) is a variant of the system developed by Hof *et al.* (2003) and, as in their case, the duration and amplitude of the perturbation can be changed independently. The injection system contained two valves with switching times of 1 ms. The rise and fall times were limited by the inertia of the small piston in the fuel injector. The quantities of fluid involved in creating the disturbance were small, and lay in the range 0.0001 % to 0.1 % of the pipe volume flux. A schematic for the specific arrangement for a single jet disturbance is shown in figure 1(*a*). The fluid was injected orthogonal to the main flow through a single hole in the pipe wall. In all, six hole diameters were used: $d = 0.5$, 1, 1.5, 2, 3 and 4 mm. A typical disturbance

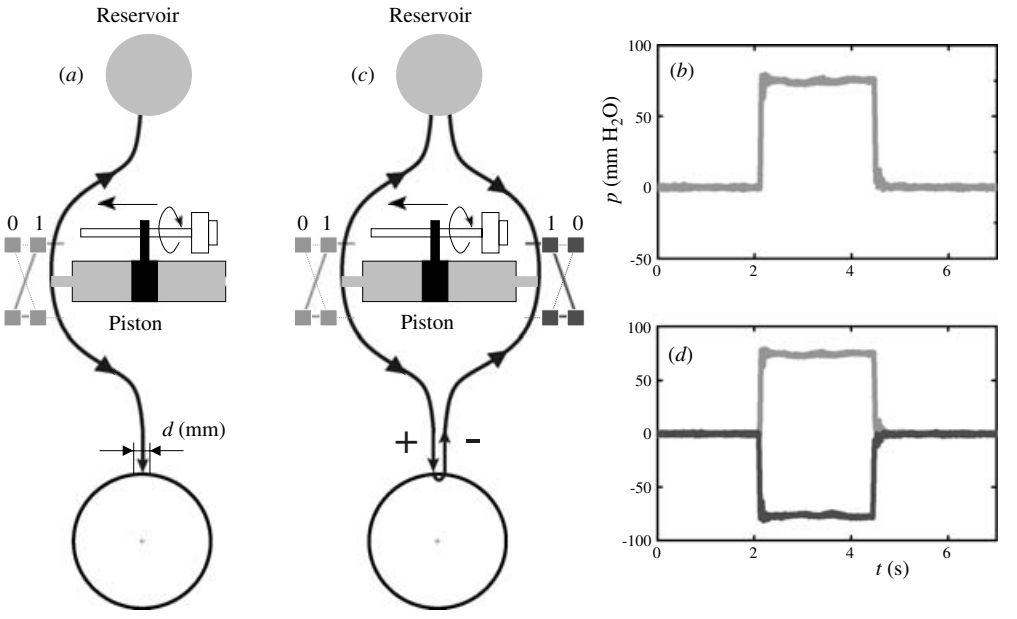

FIGURE 1. Schematics of the disturbance mechanisms and pressure trace measurements. (*a*) Single jet disturbance mechanism and (*b*) the associated pressure trace. (*c*) Push–pull disturbance mechanism and (*d*) the associated pressure traces. When the position is 0, the motor pushes (and pulls) fluid to the reservoir. When the position changes to 1, fluid is pushed (and pulled) into the pipe at a given amplitude for a given duration which is computer controlled. The amplitude is proportional to the piston velocity.

pressure trace is presented in figure 1(*b*). The displaced volume Φ_{inj} from the injector was made non-dimensional using the pipe flux Φ_{pipe} and this defined the amplitude A of the perturbation: $A = \Phi_{inj}/\Phi_{pipe}$. The duration of the injection set the spatial extent of the disturbed flow since it initially travelled at the mean flow speed. This enabled us to define a spatial scale for the disturbance which we denote by the length scale $L^* = Ut/D$ where t is the injection time.

A diagram of the push–pull mechanism and respective pressure signals are given in figures 1(*c*) and 1(*d*). This was a zero net mass flux disturbance, since an equal quantity of fluid was pushed and pulled in and out of the pipe through two 1 mm diameter holes spaced 1 mm apart. The orientation of the disturbance could be changed by rotating the alignment of the holes in order to obtain streamwise, oblique, spanwise and anti-oblique disturbances. A schematic representation of the orientation of the holes is given in figure 4.

The flow state was monitored using Mearlmaid Pearlessence as the flow visualant. A thin vertical sheet of light was formed using a series of light boxes arranged along the length of the pipe. A camera, mounted on an external traverse, was used to follow and record the flow and hence monitor the evolution of disturbances. A typical set of photographs of the evolution of a disturbance are given in figure 5.

3. Results and discussion

The results are mainly presented in the form of finite-amplitude threshold curves and can be classified in terms of the specific disturbances used to test the stability of the flow. The first set of results are concerned with the effects of the injection of

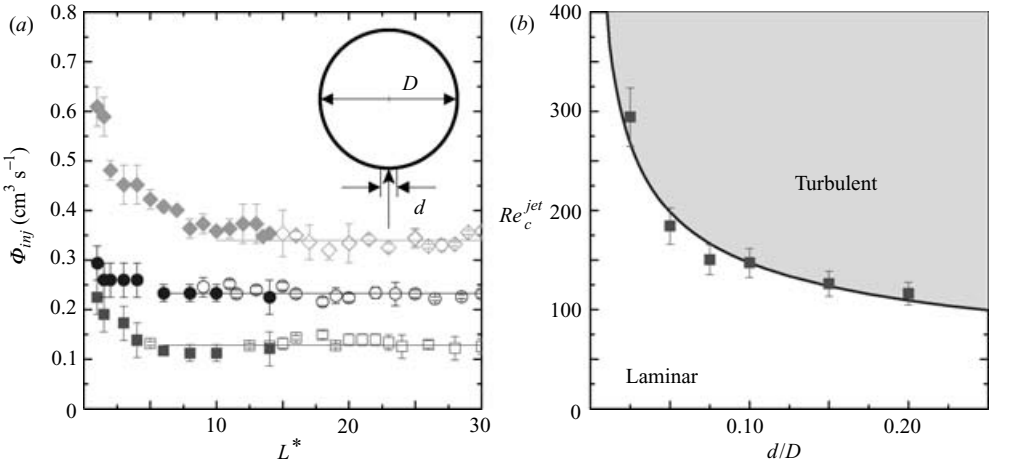

FIGURE 2. Effect of the size of the hole (*a*) Φ_{inj} versus L^* for different jet diameters (squares: $d = 0.2\ D$; circles: $d = 0.1\ D$; diamonds: $d = 0.025\ D$) for different Re (filled symbols: $Re = 2500$; open symbols $Re = 5000$) and (*b*) Re_c^{jet} versus d/D. The line is a least-squares fit $Re_c^{jet} \propto (d/D)^{-0.5}$.

small amounts of fluid across the pipe through a single hole. The dependence of the threshold level on the diameter of the hole has been investigated and comparisons have also been made with azimuthal injection through a sequence of holes. The final set of results is concerned with investigating the effects of localizing the disturbance via push–pull through a pair of holes. Hence, the perturbation contributes zero net mass flux to the main flow. A hairpin vortex structure has been revealed using this optimal configuration.

3.1. *Single jet disturbance*

The amplitude of the injected flux required to cause transition is plotted as a function of L^* in figure 2(*a*) for $Re = 2500$ and $Re = 5000$. Note we have used the dimensional form of the injected mass flux here in order to superpose the results obtained for different Re. Results are presented for three jet diameters ($d = 0.5$, 2 and 4 mm) where each data set indicates the threshold level for transition, i.e. amplitudes have to be above the respective curve to cause transition. If the duration of the perturbation was such that $L^* \lesssim 6$, a nonlinear dependence of the critical value of Φ_{inj} on L^* was obtained in agreement with Hof *et al.* (2003) and Hof (2005). However, when $L^* \gtrsim 6$, the critical disturbance amplitude is independent of L^*, but the level of the threshold depends on the diameter of the disturbance jet. We use these L^* independent threshold levels to construct figure 2(*b*) where we plot Re_c^{jet} versus the non-dimensional diameter of the jet d/D. Here, $Re^{jet} = 4\Phi_{inj}/\nu\pi d$. It can be see that $Re_c^{jet} \propto d^{-0.5}$ so that proportionally larger velocities are required to cause transition as the jet diameter is reduced.

We now use the L^* independent threshold levels obtained over a range of Re with the 4 mm jet to construct a finite-amplitude transition diagram. This is presented in figure 3 where we plot the critical values of A versus Re together with results obtained for configuration with six azimuthal jets. One conclusion we can draw is that the scaling law is independent of the details of the geometry of the jets, i.e. the same scaling is found for a single orthogonal jet and six azimuthal ones. The net injected mass flux required to cause transition is approximately a factor of two greater for

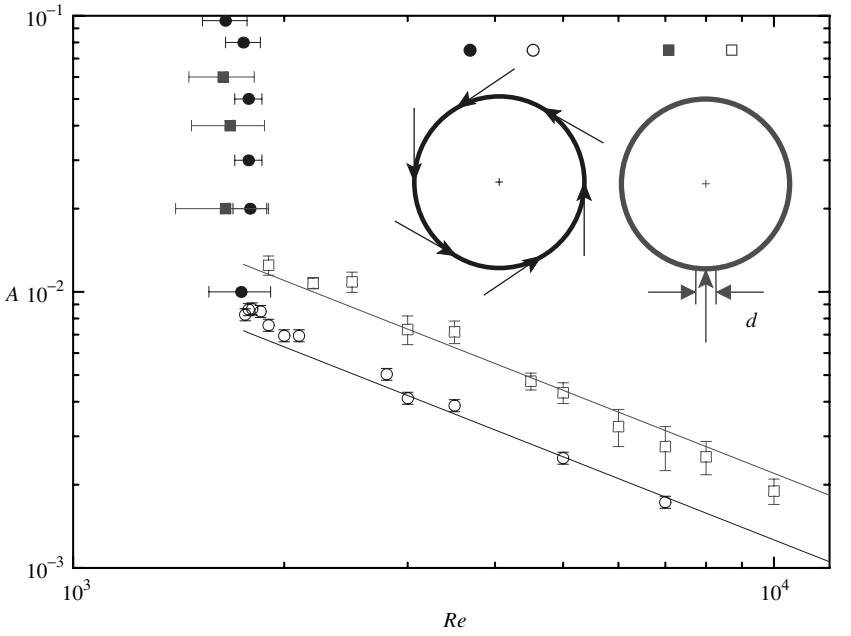

FIGURE 3. Plot of A versus Re for a single jet of diameter $d = 4$ mm (squares) and six azimuthal jets each with diameter $d = 0.5$ mm (circles). The filled symbols denote the lower bound of Re for stable puffs. They were obtained by keeping A constant and puffs relaminarized within the length of the pipe.

the single jet than for the six. Hence, the single jet is a less efficient way to achieve transition.

The estimates for the lower bound for the threshold are shown using filled symbols in figure 3. These were obtained using the method reported in Mullin & Peixinho (2005) and a sharp cutoff in the stability threshold is found. There is consistency between the data sets for both configurations. The left-hand error bar indicates rapid decay of the injected disturbance in $\lesssim 100D$ and the right-hand a 95 % persistence of the puff in excess of $500D$ from the point of injection.

3.2. *Push–pull disturbance*

The finite-amplitude thresholds for the push–pull disturbances are presented in figure 4 where we also show fits of the single jet data from figure 3 so that an immediate comparison of the threshold levels can be made. It is clear that a significantly smaller disturbance amplitude is required to cause transition with the push–pull configuration than with the single jet as the level is reduced by approximately one order of magnitude. This observation is consistent with Darbyshire & Mullin (1995). Various orientations of the push–pull disturbance were used to obtain the results in figure 4. These were spanwise, oblique, streamwise and anti-oblique, i.e. across, at 45°, in line and at 135° to the mean flow, respectively, as shown schematically in figure 4.

Each data point was obtained as a statistical average of about 40 experimental runs where the error bars denote the width of the transition threshold as discussed in §2 above. A least-squares fit to the streamwise and spanwise data gives an estimate of -1.3 ± 0.1 with a confidence limit of 93 % for the power-law dependence of A on Re.

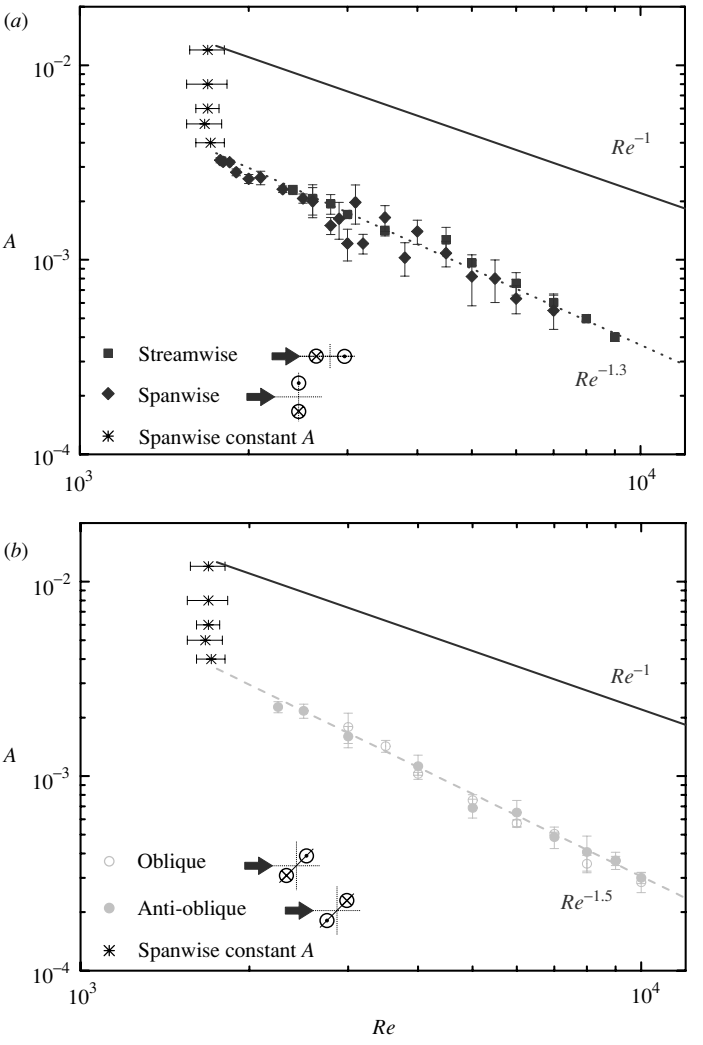

FIGURE 4. Finite-amplitude curves for the push–pull disturbance. In the schematic diagrams of the geometry of the disturbances presented in the lower left-hand corner of the figure, ⊗ indicates that fluid is pulled out of the pipe and ⊙ indicates that fluid is pushed into the pipe. (*a*) Spanwise and streamwise disturbance with a $Re^{-1.3}$ fit. Also shown is the Re^{-1} fit for the single jet data. (*b*) Oblique and anti-oblique disturbance with a $Re^{-1.5}$ fit together with the Re^{-1} fit for the single jet data.

The corresponding data for the oblique and anti-oblique data gives -1.5 ± 0.1 with a confidence limit of 99 %. Both of these relationships are significantly different from -1. They are in accord with ideas of algebraic growth as discussed by Trefethen *et al.* (1993), O'Sullivan & Breuer (1994), Grossmann (2000) and Mellibvosky & Meseguer (2006). Inertial effects are now greater than viscous dissipation so that small-amplitude perturbations can initially grow because of non-normal effects (Henningson & Kreiss 2005). Thus, we were directed towards investigating the growth phase of disturbances and the results of this are outlined in the following section.

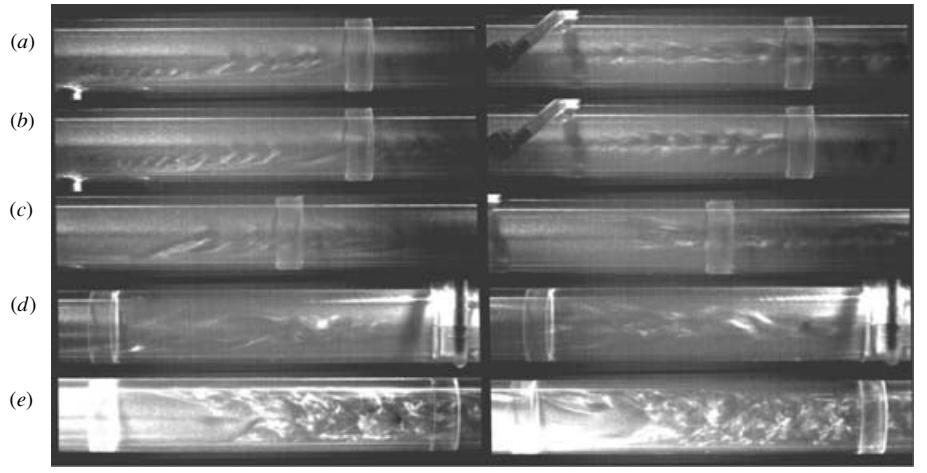

FIGURE 5. A sequence of flow-visualization images showing the development of a disturbance from the oblique push–pull perturbation with $A = 0.0023$ at $Re = 2200$. (a–e) The disturbance was injected in the plane of the photograph and (f–j) the disturbance was injected in the direction of the view. Images taken at (a, e) 0.1, (b, f) 0.2, (c, g) 0.6, (d, h) 1 and (e, i) 1.5 seconds from the beginning of the injection using a camera travelling at the same speed as the flow.

3.3. *Flow visualization*

We reinforce the above discussion on algebraic growth by showing the flow patterns associated with the development of an oblique disturbance close to the critical amplitude (figure 5). There are two sequences of flow visualization photographs. In figures 5(a) to 5(e), the disturbance was injected in the plane of the photograph and in figures 5(f) to 5(j), it was injected in the direction of the view. In all cases, the images were taken such that the small holes through which the disturbance passed, are located at the left-hand edges of each of figures 5(a), 5(b), 5(f) and 5(g) and the flow is from left to right.

The principal feature we wish to highlight, is the appearance of regular vortices which have a horseshoe-like structure (Klebanoff, Tidstrom & Sargent 1962; Acarlar & Smith 1987). Although these features are clearly nonlinear, they form part of a transition sequence and are hence different from the catastrophic events found using jets and azimuthal disturbances. Such structures have been found as secondary instabilities in the breakdown of low-speed streaks in numerical investigations of boundary-layer transition (Brandt 2007). The wavelength associated with the vortices in figure 5, is approximately $0.5D$ and is independent of Re over the range 2000 to 3000. For disturbance amplitudes less than critical, the horseshoe vortices appeared in transient form and eventually decayed as they were swept downstream. For amplitudes above the critical range, as shown here, they developed secondary structures which penetrated the central flow and transition to a puff developed rapidly. Vortices of this type have also been observed where periodic forcing was applied to pipe flow using a blowing and suction mechanism over a thin azimuthal section (van Doorne 2004) and using periodic forcing (Han, Tumin & Wygnanski 2000). However, the zero net mass flux push–pull disturbance used here requires a disturbance an order of magnitude smaller and is localized.

4. Conclusions

The stability of pipe Poiseuille flow has been tested using several finite-amplitude disturbances. The critical amplitude required to cause transition scales as Re^{-1} for single crossflow jets and arrays arranged azimuthally. These results are in agreement with Hof *et al.* (2003) and, moreover, the single jet has self-consistent behaviour. The threshold amplitude for push–pull disturbances is significantly lower than simple injection, and the scaling law exponents lie in the range -1.3 to -1.5. These are consistent with the possibility of transient growth in the initial steps of the transition process. Evidence for this has also been produced in the form of horseshoe structures using flow visualization and these are known to play a central role in boundary-layer transition as discussed by Klebanoff *et al.* (1962) and Kachanov (1994).

These new observations of a sequential transition sequence are in accord with ideas put forward by O'Sullivan & Breuer (1994). They showed evidence for transient growth in a numerical investigation of transition in a pipe and made the observation that the transient phase was more evident when small-amplitude perturbations were applied whereas it tended to be swamped for large perturbations. A convincing argument is made that the energy required to enable the growth of small perturbations is extracted from the mean flow. On the other hand, large perturbations distort the mean flow and algebraic growth is suppressed. All of the amplitudes of the perturbations used for the push–pull cases are $\lesssim 0.1$ % and this is possibly why we have been able to find this sequence.

We speculate that suction through wall may be the most significant part of the new perturbation since this will induce a favourable pressure gradient towards the wall. Hence, fast-moving fluid will be diverted from the central flow to the wall, thereby creating an inflection point in the velocity profile. Details of the subsequent transition process are, as yet, unclear and this will require an extensive quantitative investigation using particle image velocimetry. This is planned for the near future.

This research is supported by EPSRC. T. M. is supported by a Senior Fellowship and J. P. by the research grant GR/576137/01. We are grateful to R. R. Kerswell, A. Meseguer, F. Waleffe and A. P. Willis for helpful discussions and H. F. Fasel and D. S. Henningson who suggested this particular form for the push–pull perturbation.

REFERENCES

Acarlar, M. S. & Smith, C. R. 1987 A study of hairpin vortices in a laminar boundary layer. Part 2. Hairpin vortices generated by fluid injection. *J. Fluid Mech.* **175**, 43–83.

Binnie, A. M. & Fowler, J. S. 1948 A study by double-refraction method of the development of turbulence in a long circular tube. *Proc. R. Soc. Lond.* **192**, 32–44.

Brandt, L. 2007 Numerical studies of the instability and breakdown of a boundary-layer low-speed streak. *Eur. J. Mech.* B/*Fluids* **26**, 64–82.

Darbyshire, A. G. & Mullin, T. 1995 Transition to turbulence in constant-mass-flux pipe flow. *J. Fluid Mech.* **289**, 83–114.

van Doorne, C. W. H. 2004 Stereoscopic PIV on transition in pipe flow. PhD thesis, Technische Universiteit Delft.

Draad, A. A., Kuiken, G. D. C. & Nieuwstadt, F. T. M. 1998 Laminar–turbulent transition in pipe flow for Newtonian and non-Newtonian fluids. *J. Fluid Mech.* **377**, 267–312.

Drazin, P. G. & Reid, W. H. 1980 *Hydrodynamic Stability*. Cambridge University Press.

Eckhardt, B. & Mersmann, A. 1999 Transition to turbulence in a shear flow. *Phys. Rev.* E **60**, 509–517.

Faisst, H. & Eckhardt, B. 2003 Travelling waves in pipe flow. *Phys. Rev. Lett.* **91** (224502).

Govindarajan, R. & Narasimha, R. 1991 The role of residual nonturbulent disturbances on transition onset in two-dimensional boundary layers. *Trans. ASME* I: *J. Fluids Engng*. **113**, 147–149.

Grossmann, S. 2000 The onset of shear flow turbulence. *Rev. Mod. Phys*. **72**, 603–618.

Han, G., Tumin, A. & Wygnanski, I. J. 2000 Laminar–turbulent transition in Poiseuille pipe flow subjected to periodic perturbation emanating from the wall. *J. Fluid Mech*. **419**, 1–27.

Henningson, D. S. & Kreiss, G. 2005 Threshold amplitudes in subcritical shear flows. In *Proc. IUTAM Symposium Laminar–Turbulent Transition and Finite Amplitude Solutions* (ed. T. Mullin & R. Kerswell), pp. 232–245. Springer.

Hof, B. 2005 Transition to turbulence in pipe flow. In *Proc. IUTAM Symposium Laminar–Turbulent Transition and Finite Amplitude Solutions* (ed. T. Mullin & R. Kerswell), pp. 221–231. Springer.

Hof, B., Juel, A. & Mullin, T. 2003 Scaling of the turbulence transition threshold in a pipe. *Phys. Rev. Lett*. **91** (244502).

Kachanov, Y. S. 1994 Physical mechanisms of laminar–boundary-layer transition. *Annu. Rev. Fluid Mech*. **26**, 411–82.

Kerswell, R. R. 2005 Recent progress in understanding the transition to turbulence in a pipe. *Nonlinearity* **18**, 17–44.

Klebanoff, P. S., Tidstrom, K. D. & Sargent, L. M. 1962 The three-dimensional nature of boundary-layer instability. *J. Fluid Mech*. **12**, 1–34.

Leite, R. J. 1959 An experimental investigation of the stability of Poiseuille flow. *J. Fluid Mech*. **5**, 81–96.

Levin, O. 2005 Numerical studies of transition in wall-bounded flows. PhD thesis, KTH Mechanics.

Levin, O., Davidsson, E. N. & Henningson, D. S. 2005 Transition thresholds in the asymptotic suction boundary layer. *Phys. Fluids* **17** (114104).

Mellibvosky, F. & Meseguer, A. 2006 The role of streamwise perturbations in pipe flow transition. *Phys. Fluids* **18** (074104-9).

Meseguer, A. 2003 Streak breakdown instability in pipe Poiseuille flow. *Phys. Fluids* **6** (5), 1203–1213.

Mullin, T. & Peixinho, J. 2005 Recent observations of the transition to turbulence in a pipe. In *Proc. Sixth IUTAM Symposium on Laminar-Turbulent Transition* (ed. R. Govindarajan), pp. 45–55. Springer.

O'Sullivan, P. L. & Breuer, K. S. 1994 Transient growth in circular pipe flow. II Nonlinear development. *Phys. Fluids* **6** (11), 3652–64.

Peixinho, J. & Mullin, T. 2006 Decay of turbulence in pipe flow. *Phys. Rev. Lett*. **96** (094501).

Pfenniger, W. 1961 Transition in the inlet length of tubes at high Reynolds numbers. In *Boundary Layer and Flow Control* (ed. G. V. Lachman), pp. 970–980.

Reynolds, O. 1883 An experimental investigation of the circumstances which determine whether the motion of water shall be direct or sinuous and of the law of resistance in parallel channels. *Proc. R. Soc. Lond*. A **35**, 84–99.

Schmid, P. J. 2007 Nonmodal stability theory. *Annu. Rev. Fluid. Mech*. **39**, 129–162.

Schmid, P. J. & Henningson, D. S. 2001 *Stability and Transition in Shear Flows*. Springer.

Seidel, J. & Fasel, H. F. 2001 Numerical investigations of heat transfer mechanisms in the forced laminar wall jet. *J. Fluid Mech*. **442**, 191–215.

Shan, H., Zhang, Z. & Nieuwstadt, F. T. M. 1998 Direct numerical simulation of transition in pipe flow under the influence of wall disturbances. *Intl. J. Heat Fluid Flow* **19**, 320–325.

Trefethen, L. N., Trefethen, A. E., Reddy, S. C. & Driscoll, T. A. 1993 Hydrodynamic stability without eigenvalues. *Science* **261**, 578–583.

Wedin, H. & Kerswell, R. R. 2004 Exact coherent structures in pipe flow: travelling wave solutions. *J. Fluid Mech*. **508**, 333–371.

Williams, S. D. 2001 An investigation of the stability of developing pipe flow. PhD thesis, University of Manchester.

Willis, A. P. & Kerswell, R. R. 2007 Critical behavior in the relaminarization of localized turbulence in pipe flow. *Phys. Rev. Lett*. **98**, 014501.

Wygnanski, I. J. & Champagne, F. H. 1973 On transition in a pipe. Part 1. The origin of puffs and slugs and the flow in a turbulent slug. *J. Fluid Mech*. **59**, 281–351.